12014

Study of the Effects of Weathering on the Chemical Composition of a Light Crude Oil Using GC/MS GC/FID

Zhendi Wang* and Merv Fingas
Emergencies Science Division, ETC, Environment Canada, 3439 River Road, Ottawa, Ontario, Canada, K1A OH3

Abstract. Quantitative information on the weathering of spilled oil is essential to a fuller understanding of the fate and behavior of oil in the environment. Such data is also useful for spill modeling. The key to acquiring data on oil weathering is the availability of precise and reliable chemical information. Exact quantitation of compounds in the oil can provide this crucial data. In this study, the effects of weathering on the chemical composition of a light crude oil, Alberta Sweet Mix Blend (ASMB), were thoroughly investigated using GC/FID and GC/MS. Complete compositional information on the ASMB oil at various degrees of evaporation (0–45%) was obtained, and the composition and concentration changes of key components and component groupings were quantitatively correlated to evaporative loss. Two opposing effects during evaporation—one is the loss of oil components due to evaporation, and another is build-up of oil components due to volume deduction—were examined. So-called "pattern recognition" plots involving more than 100 important individual oil components and component groupings were graphically depicted, and these permitted deduction of a best set of values for quantitation of exposure to evaporative weathering. A "weathering index" concept is proposed. Relatively simple and very useful mathematical equations were derived which can be utilized to describe the weathering behavior of oil and to estimate the evaporation extent of oil.

Key words: *Crude oil, oil weathering, GC / MS, GC.*

INTRODUCTION

The weathering of spilled oil in the environment has been the subject of many research efforts in recent years. When crude oil or petroleum distillate products are accidentally released to the marine environment, they are immediately subject to a wide variety of weathering processes [1]. These processes can include: evaporation, dissolution, dispersion, photochemical oxidation, water-oil emulsification, microbial degradation, adsorption onto suspended particulate materials, sinking, and sedimentation. In the short term after an oil spill (hours to days), evaporation is the single most important and dominant weathering process and causes considerable changes in the chemical composition and physical properties of the spilled oil [2–9]. In the first few days following a spill, the loss caused by evaporation can be up to 75 and 40% of the volume of light and medium crudes, respectively. For heavy or residual oils the losses are only about 5–10% of volume [10]. The rapid loss of low-molecular-weight hydrocarbons (such as C_1 to C_{10}) can greatly reduce the biological toxicity and restrict possible adverse effects to areas near the spill site. Hence, a thorough understanding of the quantitative relationship between the weathering by evaporation and the chemical composition changes is especially important for studying the behavior and fate of spilled oil in the environment and for taking appropriate means to restore damaged resources.

Until recently, methods did not exist for

Presented at the 17th International Symposium on Capillary Chromatography and Electrophoresis, Wintergreen, Virginia, USA, May 1995.

* Author to whom correspondence should be addressed.

 CCC 1040-7685/95/060617-23

quantitation of the extent of oil evaporative weathering. The key to acquiring data on oil weathering is the availability of precise and reliable chemical information. Exact quantitation of compounds in the oil can provide this crucial data. Since there are compounds in oil which do or do not evaporate, dissolve, degrade, or photooxidize, examination of the ratios of the amounts of two compounds, and/or two compound classes, one of which does not undergo some weathering process and one of which does, can provide this key. This method is probably the only way to measure the extent of a weathering process in the case of an actual spill, and therefore, it is the method by which laboratory data and actual spill data can be correlated.

In the past decade, some laboratory experiments and field studies have been conducted to determine evaporation and measure the loss of hydrocarbons from oil. The variation in the results that have been obtained appear to be associated with different evaporation models and experimental techniques. There have been few studies in which more comprehensive and complete chemistry data are correlated to different weathering degrees.

In this report, ASMB, oil was used to study the effects of weathering on the chemical composition and concentration changes of the oil. This oil was chosen because its chemical composition has been extensively characterized and quantified [11, 12], and the oil is often used by other laboratories in Canada as a reference material for use in the comparison of analytical methods and results. The analytes include not only the toxic constituents such as alkyl benzenes, polynuclear aromatic hydrocarbons (PAH), and their alkyl homologues (which are an environmental concern), but also the major oil constituents—n-alkanes (n-C_8 to n-C_{40}) and acyclic isoprenoids, which are useful as indicators of the weathering of oil in environment, and minor (but extremely valuable in tracing and evaluating the fate of oil) constituents, such as biomarker compounds (triterpanes and steranes).

The main objectives of this study were: 1) to obtain more complete compositional information about ASMB oil at various degrees of weathering; 2) to quantitatively determine the concentrations of all monitored components at different weathering degrees, and, therefore, to compute, tabulate, and compare the composition changes and concentration changes of corresponding compounds; 3) to quantitatively examine the ratios of the amounts of compounds, and/or compound classes, which do not undergo weathering processes with those that do; and 4) to quantitatively correlate weathering percentages by evaporation with the concentration changes of the target analytes by mathematical equations, that is, to firmly base the modeling effort on complete analytical data.

The information obtained from this study will be useful for evaluating the weathering behavior and predicting the composition and concentration changes of oil in the short term following a spill. It will also be valuable for assessing the possible biological effects and the spill's damage to the environment and natural resources. This study is undertaken as part of a large effort in the Emergencies Science Division of Environment Canada and the U.S. Minerals Management Service to investigate various counter-measures in responding to oil spills and to investigate the fate and behavior of oil for both the short and long term in the environment. Further studies of the weathering effects on the chemical composition and concentration of various oils (such as medium and heavy crudes, and petroleum products as well) from different regions and studies of oil biodegradation are being conducted in this laboratory. The information obtained from further weathering studies will be combined with the information presented in this paper and used for field application and to create oil-weathering models having operational and predictive capability.

EXPERIMENTAL

Materials. The materials and standards used in this study were same as those described in references 11, 12, and 13.

Weathered ASMB oil. A new oil-evaporation technique applying a lab-scale rotary evaporator was designed and used for this purpose. The oil-weathering system consists of a Wheaton N-10 Spin Vap (Wheaton, Millville, NJ, USA) with a 10 L flask, an integral Haake F3-CH (Fisher, Attane, Canada) circulating water bath (capacity 14 L), and a Millipore vacuum pump (Millipore, Mississauga, Canada). The bath temperature can be controlled to ± 0.5°C and the thermo control range is 1–120°C. The rotation speed can be continuously varied from 10–135 rpm.

The following evaporation procedure was used to obtain weathered ASMB oils with varying weathered percentages from 0–45%: 1) fill bath with distilled water and bring to desired temperature (usually start weathering at 60°C);

2) weigh sample flask, then add approximately 2 L of ASMB crude oil into the tared roto flask, and take the final weight; 3) place flask on evaporator and run at full speed, 135 rpm. Maintain a flow of air (13 L/min) through the flask by leaving the vacuum release stopcock open; 4) after set periods of time, the sample flask is removed, reweighed and the percent evaporated (wt%) is calculated. A sample of about 5 mL is taken at approximately every ~ 5% weathering; 5) sampling is continued for about 100 h (rotovaping time), or until there is little or no change in the percentage weathered over an 8 h period.

This technique shows several advantages as follows: 1) the evaporation percentages of any target oil can be precisely controlled and then directly correlated to compositional changes of the target weathered oil; 2) by plotting weight percent lost versus time, it is possible to determine a point at which the evaporation rate is sufficiently slow that the oil may be considered to have achieved the maximum evaporative loss likely to be observed under the conditions of a marine spill; 3) it is also possible, by plotting weight percent lost versus viscosity to relate evaporative loss directly to a physical measurement which is easily obtainable in the field.

Weathered ASMB oil samples by a pan evaporation technique. The pan evaporation unit was constructed using an open pan balance (Mettler 4000) capable of measurement precision to 0.01 g. The balance is coupled to a computer for data logging. A commercial program, "Acquire," was purchased and modified to allow time intervals to be increased geometrically.

A glass evaporating pan is used. For most experiments, a single pan with a diameter of about 140 cm is used. Other diameters were used during experiments to measure the area effect. Oil of the desired weight is placed into the pan and the computer logger started. A pneumatic stirrer is put into place. This consists of a syringe with a low airflow (175 cc/min) through it. This prevents the formation of a "skin" on top of the oil, which is a major interference in these types of experiments. The "skin" formation will slow evaporation by as much as an order or two in magnitude. The experiment is run until the weight loss is very minimal. At the end of the experiment (approximately one and one-half days), the computer is manually triggered to take a final reading and the remaining oil is saved for potential future physical property and chemical composition analysis. The weight difference between the starting oil and the finished product can be measured with an accuracy of ± 0.03 grams. This yields a typical maximum error of about one part per thousand.

The oil samples with varying weathered percentages were randomly collected throughout the weathering process.

Column chromatography fractionation and capillary gas chromatography. For the instrumentation (GC-FID and GC-MS) and quantitation, please refer to references 11 and 12.

RESULTS AND DISCUSSION

Composition and concentration changes of aliphatics. Figure 1A through 1C shows the representative GC/MS chromatograms (0%, 29.8%, and 44.5%) of the m/z 85 fragment (one of the characteristic fragments for n-alkanes) of saturated hydrocarbons (F1). These chromatograms are not particularly useful for determining the source of the spill, but they provide clean traces of n-alkanes (compared to GC/FID chromatograms) in oil with minimum interference from other aliphatic hydrocarbons and give clear information on the degree of weathering or freshness of the samples, which is indicated by the distribution of n-alkane m/z 85 fragments and the hump in the bottom of the chromatograms.

Figure 1 demonstrates a number of chemical changes that occurred during the evaporation process: 1) the first major change in the oil is the loss of the relatively volatile low-molecular-weight (MW) aliphatics through evaporation; 2) build-up of less volatile high MW aliphatic components; 3) increase of the "hump" (which appears as the area between the lower baseline and the curve defining the base of resolvable peaks and is often used as an indicator of weathering degree) representing the GC unresolved hydrocarbons.

Table I summarizes quantitation results of n-alkanes from n-C_8 to n-C_{40} plus pristane and phytane in the weathered ASMB oils, as determined by using the integrated peak areas by GC/FID and internal standard method. In order to quantitatively compare the n-alkane concentration changes on the same basis, the ratios of n-alkanes relative to n-C_{30} are calculated and plotted versus carbon number (Figure 2). n-C_{30} is chosen as reference because it is well-resolved, highly evaporation-resistant, and has relatively high abundance. Figures 3A through 3F depict graphically the n-alkane distribution at varying weathering degrees.

For the source ASMB oil, the most abun-

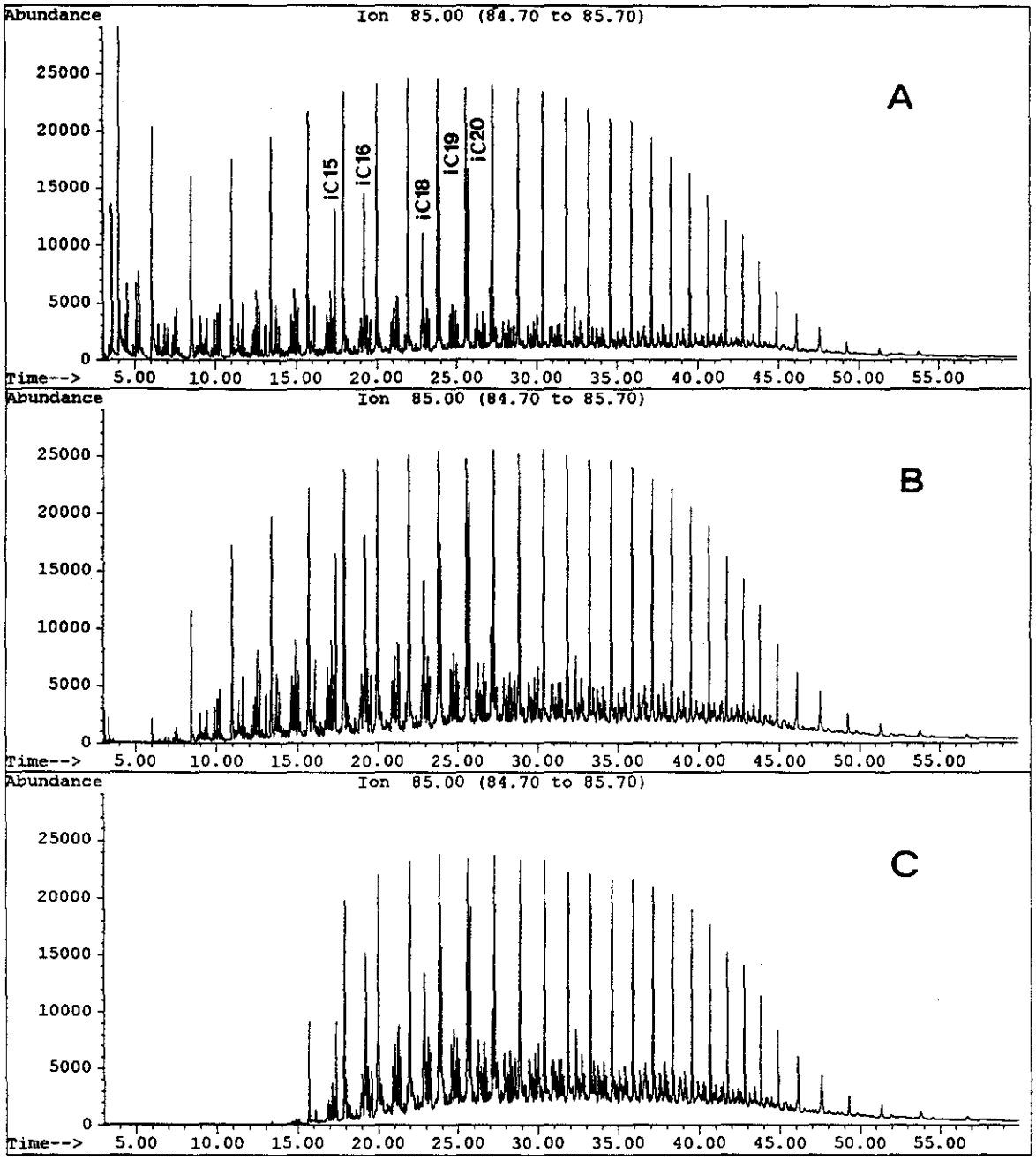

Figure 1. *GC / MS chromatograms of saturated hydrocarbons (m/z: 85) in weathered ASMB oil samples: 0%(A); 29.8% (B); and 44.5% (C). An HP-5 fused-silica column with dimensions of 30M ×0–25 mm (0–25 μm film) was used. The chromatographic conditions were as follows: carrier gas, He (1.0 mL / min); injection mode: splitless; injector and detector temperature, 290 and 300°C respectively, temperature program, 50°C for 2 min, then ramp at 6°C / min to 300°C and hold 16 min.*

dant n-alkanes are around n-C_8 to n-C_{17}, and the abundance of n-alkanes gradually decreases as the carbon number increases. As the weathered percentages increase, the most abundant aliphatic components shift to higher carbon number n-alkanes. For example, the n-alkane of the highest concentration is n-C_9 for 0% weathered oil (4.8 mg/g oil) and n-C_{17} for 44.5% weathered oil (6.7 mg/g oil), respectively. It is noted that even though the ASMB oil was weathered from 0–45%, the sum of n-alkanes for six weathered ASMB oil samples was not changed much (in the range of 70–76 mg/g oil). This can be explained as the result of the combination of two opposite effects: one is the loss of low MW aliphatic components by

Table I. *Comparison and concentration changes of aliphatics constituents in weathered ASMB oil (mg / g oil).*

n-Alkane	0%	9.8%	19.5%	29.8%	34.5%	44.5%
n-C8	4.09	2.77	1.09	0.00	0.00	0.00
n-C9	4.79	4.02	2.88	0.14	0.00	0.00
n-C10	4.35	4.12	3.53	1.36	0.08	0.00
n-C11	4.29	4.43	4.46	3.65	1.16	0.00
n-C12	4.15	4.17	4.34	4.44	3.11	0.00
n-C13	4.13	4.17	4.42	4.85	4.60	0.65
n-C14	4.18	4.16	4.58	5.15	5.13	3.02
n-C15	3.92	4.08	4.52	5.12	5.23	4.96
n-C16	3.64	4.01	4.47	4.95	5.13	5.65
n-C17	3.94	4.32	5.01	5.70	5.78	6.73
Pristane	1.96	2.11	2.35	2.71	2.80	3.13
n-C18	3.28	3.51	4.08	4.72	4.76	5.72
Phytane	1.92	2.05	2.33	2.70	2.73	3.20
n-C19	2.56	2.74	3.10	3.48	3.82	4.54
n-C20	2.30	2.47	2.80	3.12	3.39	4.02
n-C21	2.21	2.36	2.65	2.98	3.26	3.93
n-C22	2.03	2.23	2.55	2.84	3.00	3.57
n-C23	1.78	2.01	2.30	2.53	2.71	3.14
n-C24	1.70	1.85	2.23	2.45	2.62	3.05
n-C25	1.56	1.61	1.89	2.08	2.24	2.69
n-C26	1.38	1.54	1.78	2.04	2.14	2.54
n-C27	1.27	1.43	1.65	1.85	1.99	2.34
n-C28	1.09	1.20	1.42	1.59	1.71	1.98
n-C29	0.90	0.99	1.15	1.30	1.41	1.65
n-C30	0.72	0.77	0.94	1.05	1.12	1.31
n-C31	0.62	0.67	0.76	0.91	0.96	1.16
n-C32	0.49	0.53	0.65	0.71	0.76	0.91
n-C33	0.32	0.36	0.41	0.47	0.50	0.62
n-C34	0.28	0.32	0.37	0.41	0.44	0.53
n-C35	0.19	0.22	0.25	0.28	0.30	0.37
n-C36	0.12	0.14	0.16	0.18	0.19	0.22
n-C37	0.09	0.10	0.12	0.14	0.13	0.15
n-C38	0.06	0.07	0.08	0.09	0.10	0.12
n-C39	0.05	0.06	0.07	0.07	0.08	0.10
n-C40	0.04	0.04	0.05	0.06	0.06	0.07
Sum	70.30	71.69	75.64	75.91	73.77	72.58
n-C17/pristane	2.02	2.05	2.13	2.10	2.07	2.15
n-C18/phytane	1.71	1.71	1.75	1.75	1.78	1.78
pristane/phytane	1.02	1.03	1.01	1.00	1.03	0.98
CPI*	0.96	0.99	1.02	1.00	1.01	1.01
(C8+C10+C12+C14)/ (C22+C24+C26+C28)	2.70	2.23	1.70	1.23	0.88	0.27

*CPI: Carbon Preference Index = (sum of odd n-alkanes)/(sum of even n-alkanes).

evaporation, and another is the buildup of high MW aliphatic components by oil volume reduction. The ratios of n-C_{17}/pristane, n-C_{18}/phytane, and pristane/phytane are virtually unaltered (see Table I) because these compounds have about the same volatility. The values of carbon preference index (CPI), defined as the sum of odd n-alkanes over the sum of even n-alkanes, are found to be around 1.0 for all samples, which is a characteristic indication of petroleum. It can be clearly seen from Figure 2 that from n-C_{20} to n-C_{22}, all data points from six weathered oils converge, indicating that relative to n-C_{30}, the high MW n-alkanes (e.g., > C_{22}) are virtually unaffected by evaporation. The variability in fraction 1 is primarily in proportion to low MW aliphatics which are most susceptible to evaporation.

Based on the quantitation results, a mathematical equation has been developed to quanti-

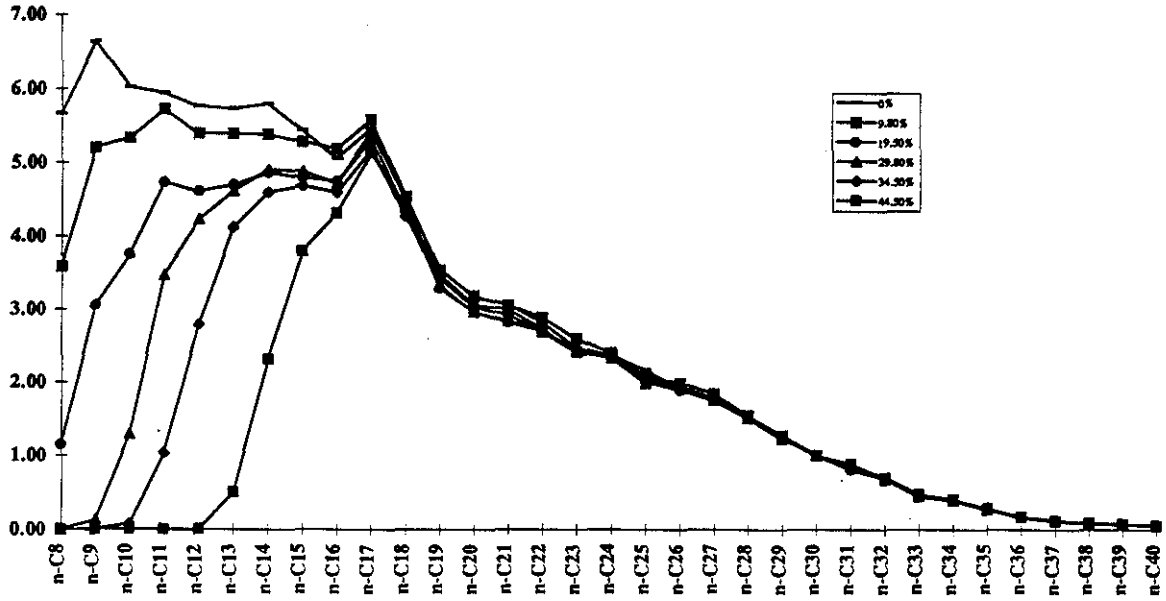

Figure 2. *Plots of abundances of n-alkane in weathered ASMB oil samples relative to n-C_{30}.*

tatively describe the correlation of oil component concentrations to the percentages lost by evaporation as follows:

$$C_{conv} = C_{det}(1 - P) \qquad (1)$$

where C_{conv} is defined as converted concentrations of oil components in weathered samples, which is equivalent to the concentrations in the source oil; C_{det} = concentrations of oil components in weathered samples determined from GC analyses; P = weathered percentages of oil by weight (%).

Based on Equation 1, the converted concentrations of n-alkanes can be readily obtained using the data listed in Table I. Figure 4 compares plots of C_{det} (4A, top) and C_{conv} (4B, bottom) of several selected n-alkanes (n-C_{10}, n-C_{12}, n-C_{16}, n-C_{20}, n-C_{25}, and n-C_{30}) versus evaporation percentages.

As described above, there are two opposing factors which affect the concentration changes of oil components during the evaporation process: the first factor is evaporation, which results in the concentration decrease of oil components; the second is volume reduction by evaporation, which results in the concentration increase of oil components. The importance of equation (1) is that it eliminates the effect of volume reduction and focuses the effect of evaporation on the oil component concentration changes. Thus, the composition and concentration changes are compared on an equal basis. Figure 4A reflects the combined effects of evaporation and volume reduction of oil aliphatics, while Figure 4B directly reflects the effect of the single factor evaporation on the composition changes, based on the assumption that the oil volume was not altered during the weathering process. For example, the plots of the measured concentration of n-C_{16}, n-C_{20}, n-C_{25}, and n-C_{30} versus weathered percentage are all upward, as shown in Figure 4A; however, after the effect of the volume reduction is eliminated, the slope of n-C_{16} becomes downward and the plots of n-C_{20}, n-C_{25}, and n-C_{30} are parallel to the x-axis, indicating that the concentration of n-C_{16} has actually decreased, while the concentrations of n-C_{20}, n-C_{25}, and n-C_{30} are almost unchanged. Figure 4B clearly demonstrates that: 1) from C_8 to C_{22}, the evaporation rate is a function of carbon chain length with shorter chain n-alkanes decreasing in concentration more rapidly than longer n-alkanes; 2) n-alkanes with carbon number greater than 22 are virtually not lost by evaporation; 3) n-C_8, n-C_9, and n-C_{10} to n-C_{12} are completely lost as the evaporation percentages approach 30%, 35%, and 45%, respectively; 4) pristane and phytane show small evaporative loss as well, in approximately the same rates as n-C_{17} and n-C_{18}.

Based on the findings discussed above, a weathering index (WI) by evaporation (equation 2), defined as the concentration sum of n-C_8, n-C_{10}, n-C_{12}, and n-C_{14} divided by the

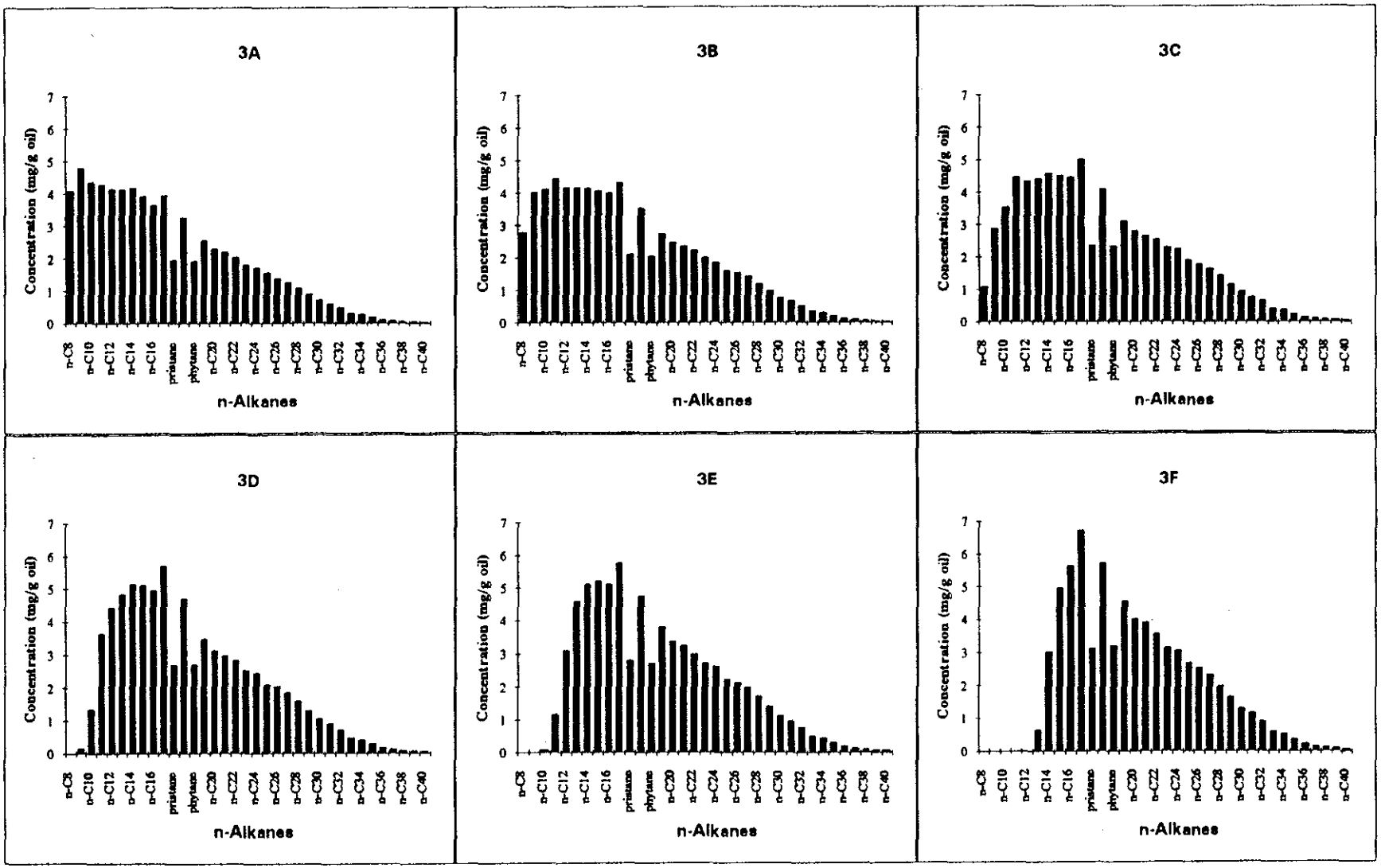

Figure 3. *n-alkane distribution in six weathered ASMB oil samples: 0% (3A); 9.8% (3B); 19.5% (3C); 29.8%(3D); 34.5% (3E); and 44.5% (3F).*

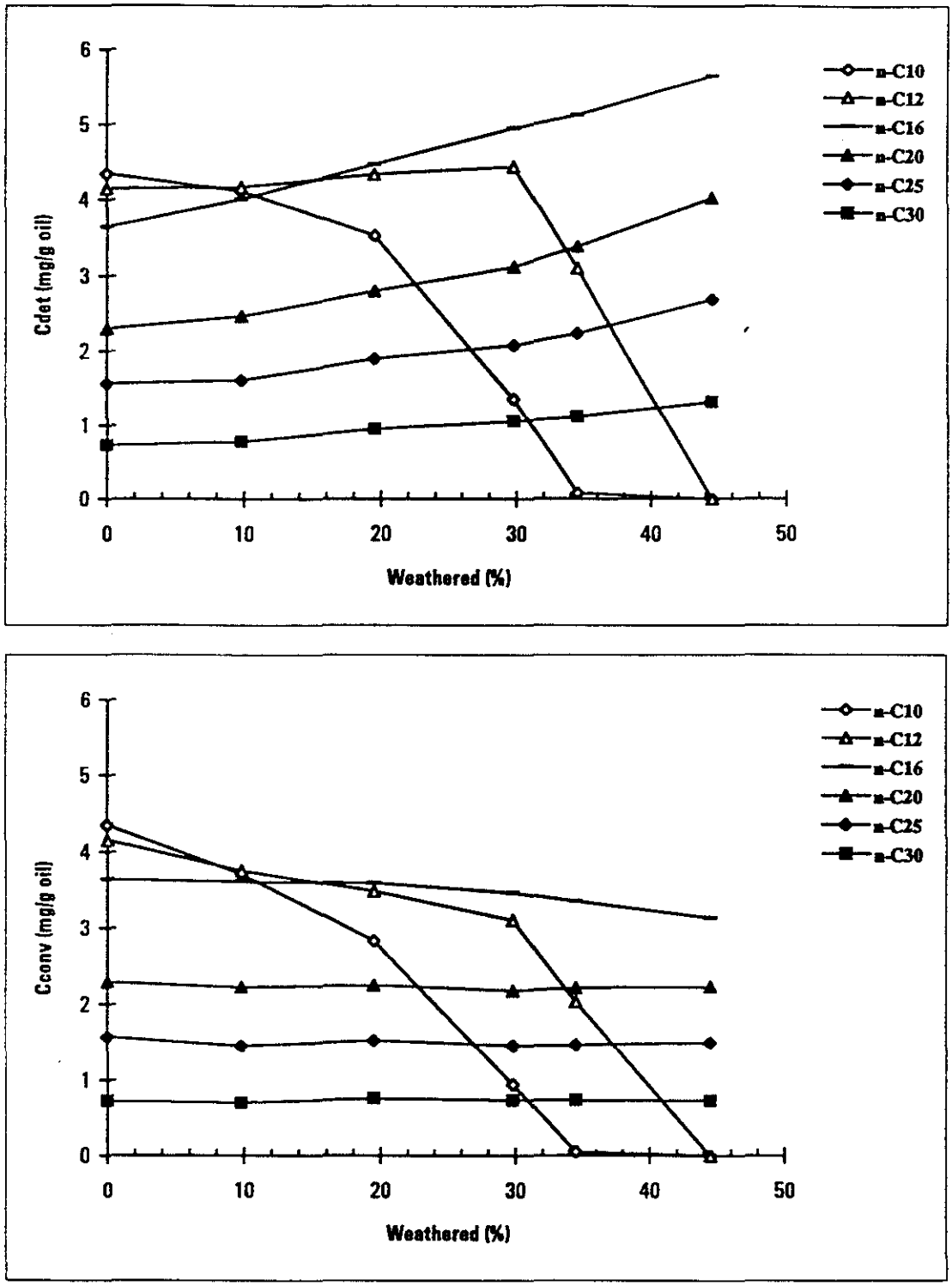

Figure 4. *Comparison of plots of C_{det} (top) and C_{conv} (bottom) versus weathered percentages for selected n-alkanes in ASMB oils.*

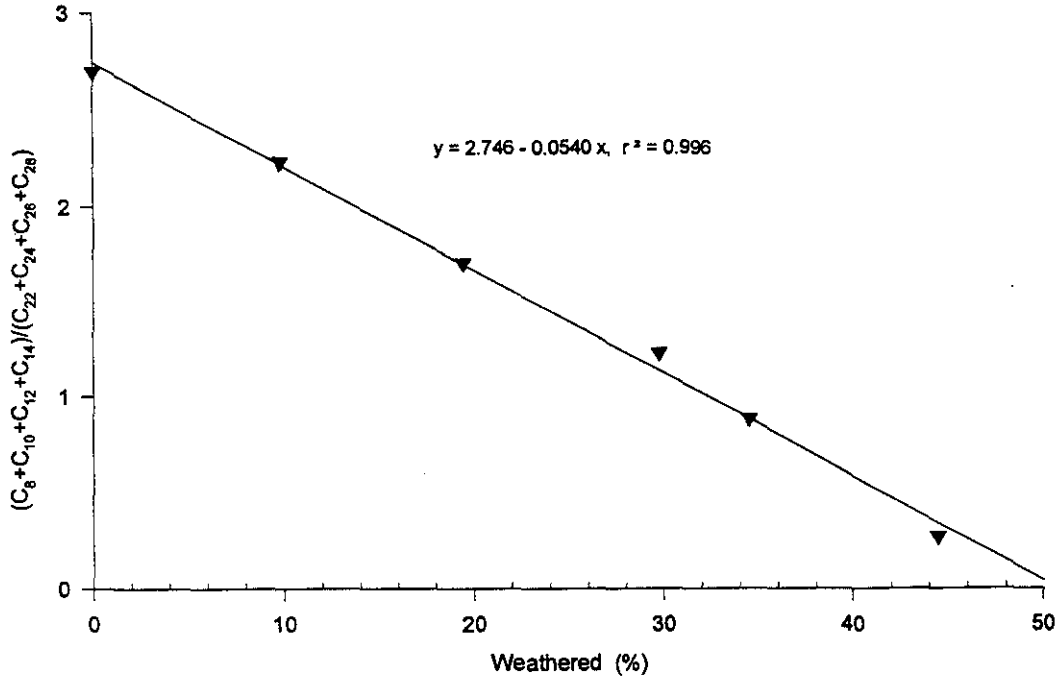

Figure 5. *Plot of weathering index* $(C_9 + C_{10} + C_{12} + C_{14})/(C_{22} + C_{24} + C_{26} + C_{28})$ *versus oil weathered percentages.*

sum of n-C_{22}, n-C_{24}, n-C_{26}, and n-C_{28}, is introduced to describe the weathering behavior of oil and to evaluate the evaporation degrees of real samples (note: this equation can be expanded to include n-C_{16} and n-C_{30}, if desired):

$$\text{WI} = (\text{n-C}_8 + \text{n-C}_{10} + \text{n-C}_{12} + \text{n-C}_{14})/(\text{n-C}_{22} + \text{n-C}_{24} + \text{n-C}_{26} + \text{n-C}_{28}). \quad (2)$$

Clearly, the value of WI is sensitive to the changes of weathering degree. As the weathered percentages increase, the value of the numerator significantly decreases and the denominator, in contrast, grows larger. A significant feature of using equation (2) is that the select ed eight n-alkanes are well resolved and have relatively high abundances, therefore the ratio can be accurately determined. The values determined according to equation (2) are 2.70, 2.23, 1.70, 1.23, 0.88, and 0.27 for the six standard weathered samples, respectively. For samples in which the low-boiling saturated hydrocarbons n-C_8 to n-C_{14} are completely lost, the WI approaches zero. If the weathering indices are drawn against the weathered percentages, a straight line is obtained (see Figure 5). Figure 5 can be used to estimate the weathering extent and degree of actual oil samples through the preferential depletion of n-C_8 to n-C_{14} relative to virtually undepleted n-C_{22} to n-C_{28}. For example, Equation 2 has been successfully used to estimate the weathering degrees of oil burn residues from the 1993 Newfoundland Offshore Burn Experiment (NOBE) [14].

Composition and concentration changes of aromatics. Figures 6A, 6B, and 6C show the GC/MS TIC chromatograms (in SIM mode) of the aromatic fraction (F2) of 0%, 29.8%, and 45% weathered ASMB oil samples. Table II summarizes the quantitation results of alkylated PAH in 6 weathered ASMB oils (the identification and quantitation results of alkyl benzenes have been reported elsewhere [15]). For comparison purposes, the converted PAH data obtained using Equation 1 are also shown in Table II (right side). Figures 7A through 7F depict the target alkylated PAH distributions. The relative compositions of target PAH in each group are listed in Table III. The decrease of the relative composition percents of C_0- and C_1-napthalenes as the weathering percentage increases are the most pronounced among the 5 alkyl PAH groups (from 7.7 and 19.3% decreased to 0 and 2.4%, respectively).

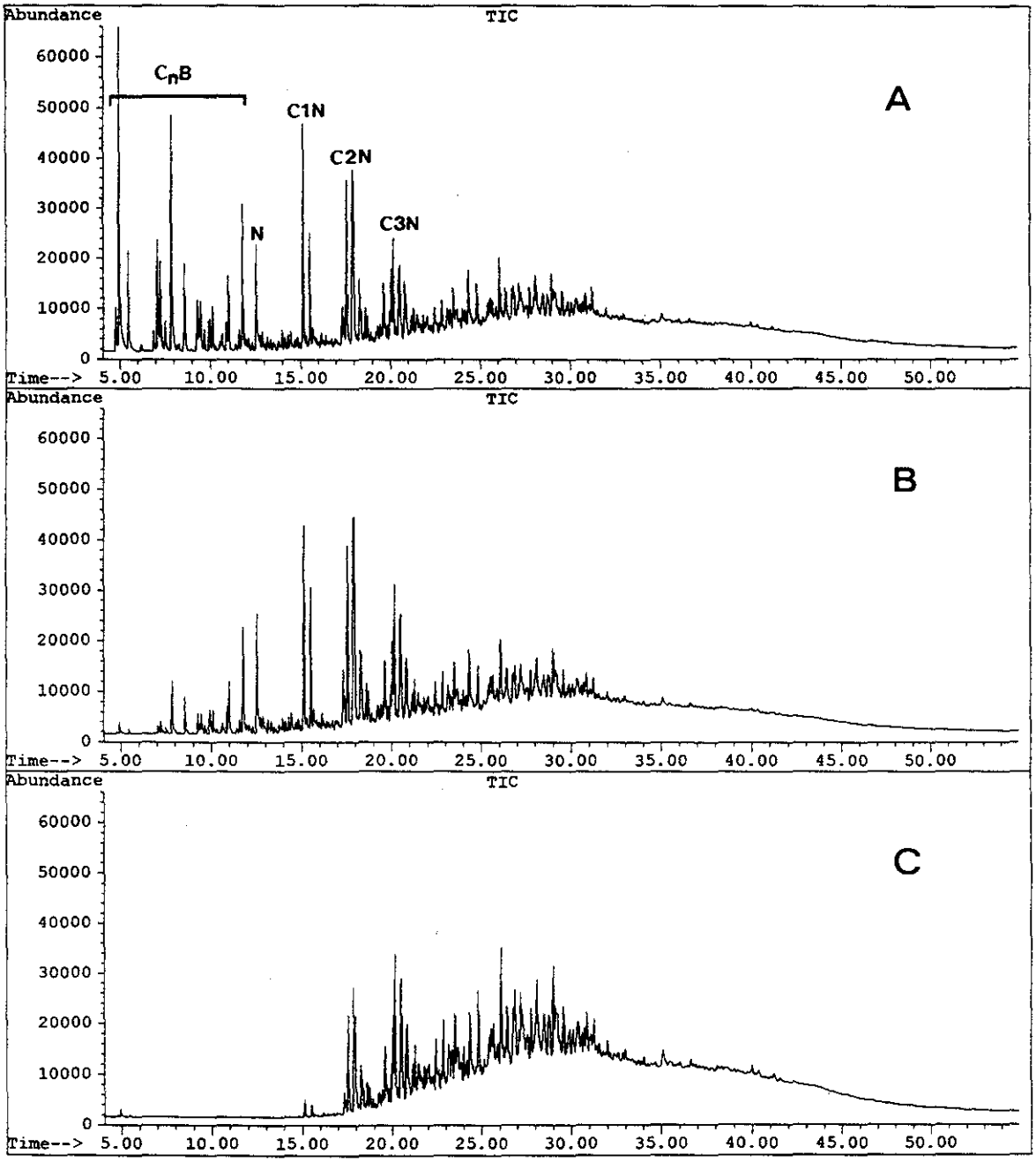

Figure 6. *GC / MS chromatograms of aromatic compounds (F2) in ASMB oil at weathered percentages 0% (A), 29.8% (B), and 44.5% (C), C_nB, N, C1N, C2N, C3N represent alkyl benzenes, naphthalene, and alkylated naphthalenes. Chromatographic conditions are same as Figure 1.*

The major compositional changes of PAH as the weathering percentage increases are summarized as follows.

1. A significant feature of the early eluted alkylated benzene (1 ring) series is their high abundance, especially the C_2-benzenes and C_3-benzenes, in comparison with PAHs (Figure 6A). As the weathering percentage increases, the concentration of alkyl benzenes dramatically decreases (Figure 6B).
2. When the evaporative percentage increases from 0 to 45%, the low-boiling alkyl benzenes with a retention time less than ~ 14 min were completely lost (Figure 6C).
3. Pronounced decrease in naphthalene and alkyl naphthalenes relative to other PAHs.

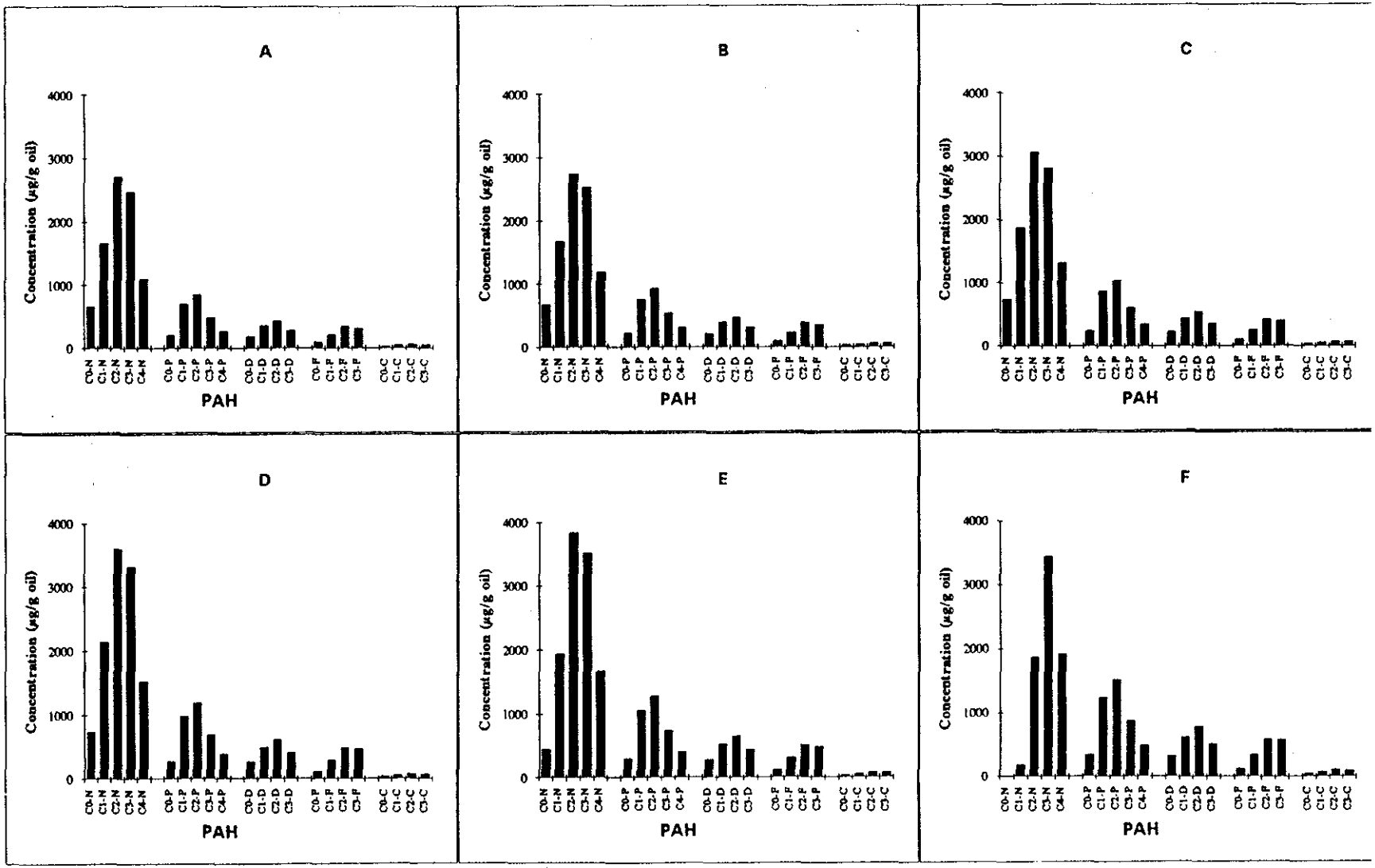

Figure 7. *Distribution of target alkylated PAH series at six weathering percentages: 0% (A); 9.8% (B); 19.5% (C); 29.8% (D); 34.5% (E); and 44.5% (F). N, P, D, F, and C represent naphthalene, phenanthrene, dibenzothiophene, fluorene and chrysene, respectively; 0, 1, 2, 3, and 4 represent carbon numbers of alkyl groups in alkylated PAH.*

Table II. *Measured (left side) and converted (right side) concentrations of target PAH in weathered ASMB oil (μg / g oil)*.*

PAH	Determined concentration (C_{det})						Converted concentration (C_{conv})					
	0.0%	9.8%	19.5%	29.8%	34.5%	44.5%	0.0%	9.8%	19.5%	29.8%	34.5%	44.5%
C0-N	660	6701	738	736	442	0	660	604	594	515	290	0
C1-N	1660	1668	1867	2137	1929	181	1660	1505	1503	1496	1263	100
C2-N	2704	2737	3070	3605	3830	1861	2704	2469	2471	2524	2508	1033
C3-N	2470	2527	2810	3320	3520	3439	2470	2279	2262	2324	2306	1909
C4-N	1095	1177	1311	1524	1666	1914	1095	1062	1055	1067	1091	1062
SUM	8589	8779	9796	11322	11387	7395	8589	7919	7886	7925	7458	4104
C0-P	197	216	237	272	294	338	197	195	191	190	193	188
C1-P	698	756	864	981	1054	1240	698	682	696	687	690	688
C2-P	843	923	1036	1188	1284	1515	843	833	834	832	841	841
C3-P	484	537	604	687	734	873	484	484	486	481	481	485
C4-P	272	311	344	389	408	487	272	281	277	272	267	270
SUM	2494	2743	3085	3517	3774	4453	2494	2474	2483	2462	2472	2471
C0-D	188	210	230	262	285	322	188	189	185	183	187	179
C1-D	352	395	438	490	531	623	352	356	353	343	348	346
C2-D	427	473	534	610	651	780	427	427	430	427	426	433
C3-D	280	315	350	405	435	504	280	284	282	284	285	280

Table II. *(Continued)*

PAH	Determined concentration (C_{det})						Converted concentration (C_{conv})					
	0.0%	9.8%	19.5%	29.8%	34.5%	44.5%	0.0%	9.8%	19.5%	29.8%	34.5%	44.5%
SUM	1247	1393	1552	1767	1902	2229	1247	1256	1249	1237	1246	1237
C0-F	89	93	104	116	120	122	89	84	84	81	79	68
C1-F	210	230	254	292	310	336	210	207	204	204	203	186
C2-F	345	384	421	481	510	592	345	346	339	337	334	329
C3-F	315	355	392	460	479	578	315	320	316	322	314	321
SUM	959	1062	1171	1349	1419	1628	959	958	943	944	929	904
C0-C	24	29	32	36	39	46	24	26	26	25	26	26
C1-C	37	42	47	53	56	67	37	38	38	37	37	37
C2-C	55	62	70	77	83	101	55	56	56	54	54	56
C3-C	54	61	66	74	77	91	54	55	53	52	50	51
Sum	170	194	215	240	255	305	170	175	173	168	167	169
Total	13459	14171	15819	18195	18737	16010	13459	12782	12734	12737	12272	8886
2-M-N/1M-N	1.35	1.38	1.35	1.32	1.31	0.99						
4-M-D/2-M-D /1-M-D	1.00:0.77:0.28	1.00:0.76:0.29	1.00:0.76:0.28	1.00:0.76:0.28	1.00:0.76:0.28	1.00:0.78:0.29						

*N, P, D, F, and C represent naphthalene, phenanthrene, dibenzothiophene, fluorene, and chrysene, respectively.

Table III. *Relative composition (%) target PAH at various weathered percentages of ASMB oil.*

PAHS	0%	9.8%	19.5%	29.8%	34.5%	44.5%
C0-N	7.7	7.6	7.5	6.5	3.9	0.0
C1-N	19.3	19.0	19.1	18.9	16.9	2.4
C2-N	31.5	31.2	31.3	31.8	33.6	25.2
C3-N	28.8	28.8	28.7	29.3	30.9	46.5
C4-N	12.7	13.4	13.4	13.5	14.6	25.9
C0-P	7.9	7.9	7.7	7.7	7.8	7.6
C1-P	28.0	27.6	28.0	0.3	27.9	27.9
C2-P	33.8	33.6	33.6	33.8	34.0	34.0
C3-P	19.4	19.6	19.6	19.5	19.4	19.6
C4-P	10.9	11.3	11.2	11.1	10.8	10.9
C0-D	15.1	15.1	14.8	14.8	15.0	14.4
C1-D	28.2	28.4	28.2	27.7	27.9	27.9
C2-D	34.2	34.0	34.4	34.5	34.2	35.0
C3-D	22.5	22.6	22.6	22.9	22.9	22.6
C0-F	9.3	8.8	8.9	8.6	8.5	7.5
C1-F	21.9	21.7	21.7	21.6	21.8	20.6
C2-F	36.0	36.2	36.0	35.7	35.9	36.4
C3-F	32.8	33.4	33.5	34.1	33.8	35.5
C0-C	14.1	14.9	14.9	15.0	15.3	15.1
C1-C	21.8	21.6	21.9	22.1	22.0	22.0
C2-C	32.4	32.0	32.6	32.1	32.5	33.1
C3-C	31.8	31.4	30.7	30.8	30.2	29.8

*N, P, D, and C represent naphthalene, phenanthrene, dibenzothiophene, fluorene, and chrysene, respectively.

Among the 5 target alkylated PAH families, the most abundant alkyl naphthalenes (2-rings) are the most easily evaporated, followed by alkyl fluorenes (3 rings, 13 carbons), and dibenzothiophenes (3-rings, 14 carbons). In general, the larger the number of rings, the more stable the compounds.

4. Most alkyl groups show the same evaporation trend: $C_0 > C_1 > C_2 > C_3 > C_4$.
5. No loss of alkyl chrysenes (4 rings) due to evaporation was observed, and they exhibit the most pronounced relative increase in abundance due to the lowest vapor pressures and the highest resistance to degradation among the 5 target alkylated PAH families [13, 16].
6. No noticeable loss by evaporation was observed for C_2-, C_3-, and C_4-phenanthrenes, C_2-and C_3-dibenzothiophenes and fluorenes.
7. For methyl-naphthalenes, the isomeric ratio of 2-methyl-naphthalene (2-M-N) to 1-methyl-naphthalene (1-M-N) was similar (2-M-N : 1-M-N = 1.3, Table II) in all but the most heavily weathered residue (44.5%) where the naphthalene was completely lost and the 1-M-N was preferentially preserved (2-M-N : 1-M-N = 0.99).
8. One of the most pronounced features of the extracted ion profile is that the methyl-dibenzothiophenes (M-D) show three well-resolved isomer peaks. They are identified as 4-M-D, 2-/3-M-D, and 1-M-D [12]. It is noted that the isomeric distribution within the C_1-dibenzothiophenes exhibits great consistency in their relative ratio (1.00 : 0.76 : 0.28, Table II) for 6 weathered oils. This feature can be used for oil differentiation and source identification [17].

In order to compare the PAH concentration changes on the same basis, Figures 8A through 8F plot C_{det} and C_{conv} of alkyl naphthalenes (Figures 8A and 8B), alkyl phenanthrenes, and alkyl fluorenes versus the weathered percentages, respectively. It can be seen from Figure 8 that the gradual build-up in the relative abundances of alkyl phenanthrene and alkyl fluorene series is obvious (Figures 8C and 8E), while alkyl naphthalenes (Figures 8A) show some complicated trends as the combined results of two opposing effects on their concentration changes (decrease in concentration due to evaporation loss, and increase in concentration due to volume reduction). In contrast, Figures 8B, 8D, and 8F are clear and simple: (1) the slope of the naphthalene plot is signifi-

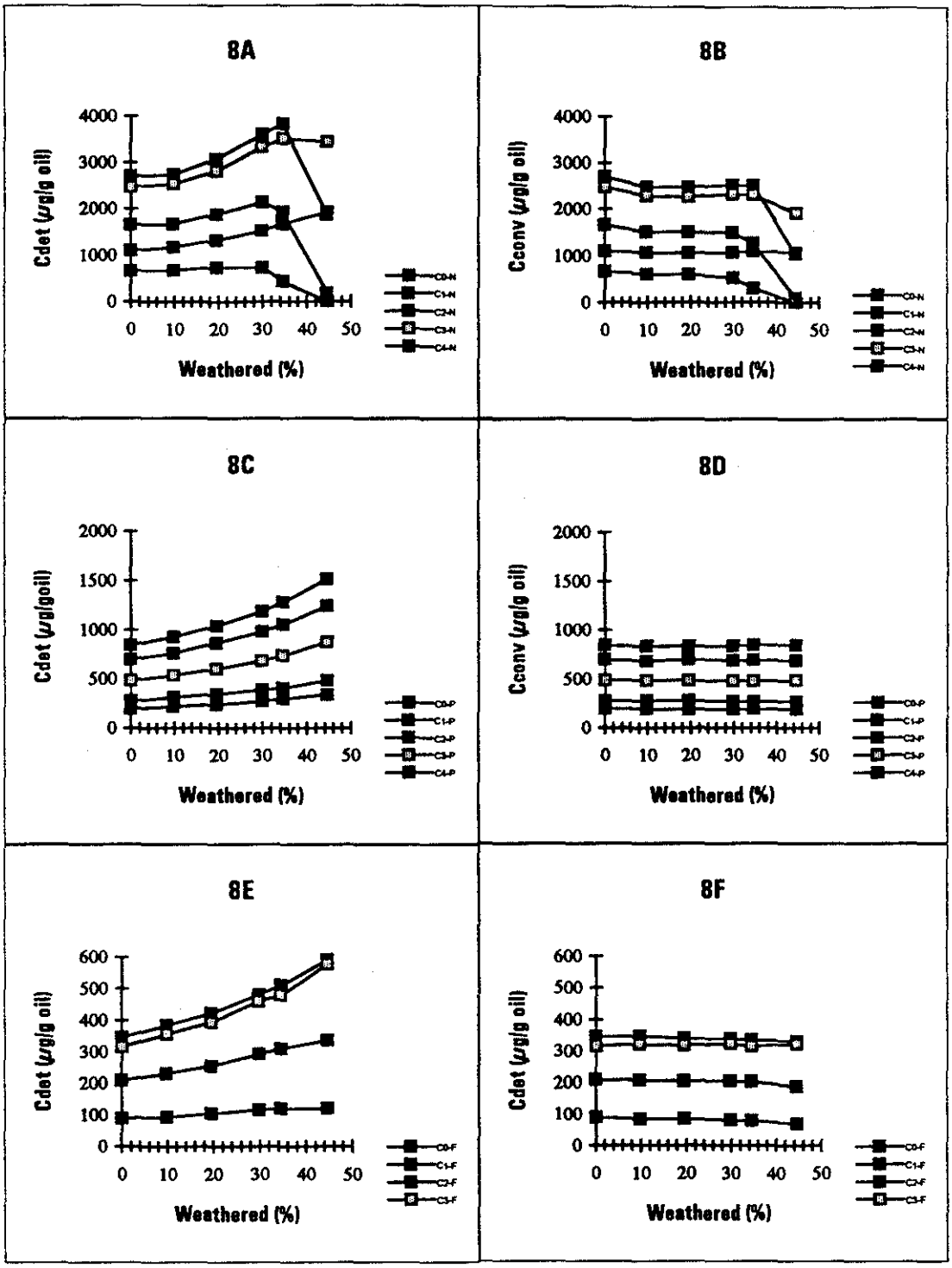

Figure 8. *Plots of C_{det} and C_{conv} versus weathered percentages of alkylated naphthalenes, (A and B), alkylated phenanthrenes (C and D), and alkylated fluorenes (E and F).*

cantly negative, indicating that its concentration decreases rapidly as the weathered percentage increases; (2) the alkyl naphthalene series and alkyl fluorene series, with the exception of C_4-naphthalenes and C3-fluorenes (they are almost parallel to x-axis), exhibit downward trends in the order of $C_4 < C_3 < C_2 < C_1 < C_0$, which means the alkyl naphthalene and fluorene series have the evaporation order of $C_0 > C_1 > C_2 > C_3 > C_4$; (3) phenanthrene

only shows small evaporative loss; (4) the plots of C_2-P, C_3-P, C_4-P, C_2-F, and C_3-F are parallel to the x-axis, indicating these components are virtually not lost by evaporation.

Composition and concentration changes of biomarker compounds. Studies on separation and identification of biomarker compounds in oil samples have greatly increased in recent years [13, 16, 18–26]. This is because the biomarkers are useful in identification of oil sources and in oil/oil correlations. Among the various types of biomarkers, triterpanes and steranes are most often used for source identification due to their high molecular weights and relatively high concentrations in crude oil. It has been found that hopane triterpane series have a high resistance to microbial degradation in comparison to many other aliphatic and aromatic compounds. Hence, the analysis of hopanes provides another valuable means of estimating oil depletion, especially for highly weathered oils which have undergone not only evaporative weathering but also biodegradation, photo-oxidation, and other kinds of degradation.

Common features of the electron impact mass spectra of many triterpanes and steranes are a relatively large parent ion, an important parent minus a methyl ion, and a basepeak at m/z 191 and 217 respectively. The triterpanes in ASMB oil are distributed over a wide range from C_{19} to C_{35} with a series of C_{19}-C_{26} tricyclic terpanes and various pentacyclic hopanes being quite prominent. As examples, Figures 9 and 10 show the GC/MS chromatograms of the triterpane distribution (9A and 9B) and sterane distribution (10A and 10B) for 0 and 44.5% weathered ASMB oil samples, respectively.

Figures 9 and 10 suggest that weathering has not altered the overall pattern and profile of the hopane and sterane distribution at all. Gradual buildups in the relative abundances of hopane and steranes from 0 to 45% weathered samples are apparent. Even by eyeball comparison, it can be readily seen from Figure 9 that the intensities of hopanes relative to the internal standard, C_{30}-$\beta\beta$-hopane, for 45% weathered oil are significantly higher than 0% weathered oil.

The detailed quantitation results for triterpanes and steranes are presented in Tables IV and V respectively. The converted concentrations for triterpanes and steranes calculated from equation (1) are virtually constant and do not indicate any evaporation. The sums of the measured concentrations (C_{det}) of triterpanes for six weathered oil samples are 992, 1074, 1195, 1325, 1428, and 1742 μg/g oil, respectively; while the corresponding sums of the converted concentrations (C_{conv}), in contrast, are 991, 968, 962, 928, 935, and 967 μg/g oil, showing very good consistency. Plotting the converted concentrations of the representative compounds C_{23}, C_{24}, Ts (18α(H), 21β(H)-22, 29, 30-trisnorhopane), Tm (17α(H), 21β(H)-22, 29, 30-trisnorhopane), C_{29} $\alpha\beta$-, and C_{30} $\alpha\beta$-hopanes against the weathered percentages, lines parallel to the x-axis are obtained. Table VI summarizes relative ratios of tricyclic triterpanes, pentacyclic hopanes, and C_{27} to C_{29} steranes. The most striking feature from Table 6 is that both hopanes and steranes show a great consistency in the relative ratios of paired biomarker compounds and/or biomarker compound classes. For example, the ratios of the paired hopanes C_{23}/C_{24}, Ts/Tm, and $C_{29}\alpha\beta/C_{30}\alpha\beta$ for six weathered oil samples are all around 2.0, 0.79, and 0.67, respectively; and the isomeric ratios (20S/(20S + 20R)) within C_{27}, C_{28}, and C_{29} sterane series are all around 0.39, 0.57, and 0.47, respectively.

A general conclusion drawn from study of the effect of evaporation on the relative chemical composition of biomarker compounds is that tricyclic and tetracyclic triterpanes, C_{27} to C_{35} hopanes, regular steranes and rearranged diasteranes were unaltered during the evaporation weathering process. A GC/MS method using biomarker compounds using especially the relative abundance ratio of C_{29}/C_{30} hopanes to characterize the 22-year-old spilled Arrow oil has been developed in this laboratory [13]. The facts found from this study demonstrate the uniqueness and usefulness of biomarker compounds for identification and characterization of long-term weathered oil samples.

Determination of evaporation percentages of weathered oil samples. Equation 1 can be rewritten in the form as shown in Equation 3:

$$P(\%) = (1\text{-}C_s/C_w) \times 100 \qquad (3)$$

where: C_w = the concentration of selected compounds in the weathered samples, which do not undergo weathering;
C_s = the concentrations of the corresponding compounds in the source oil;
P = weathered percentages of the weathered samples by weight.

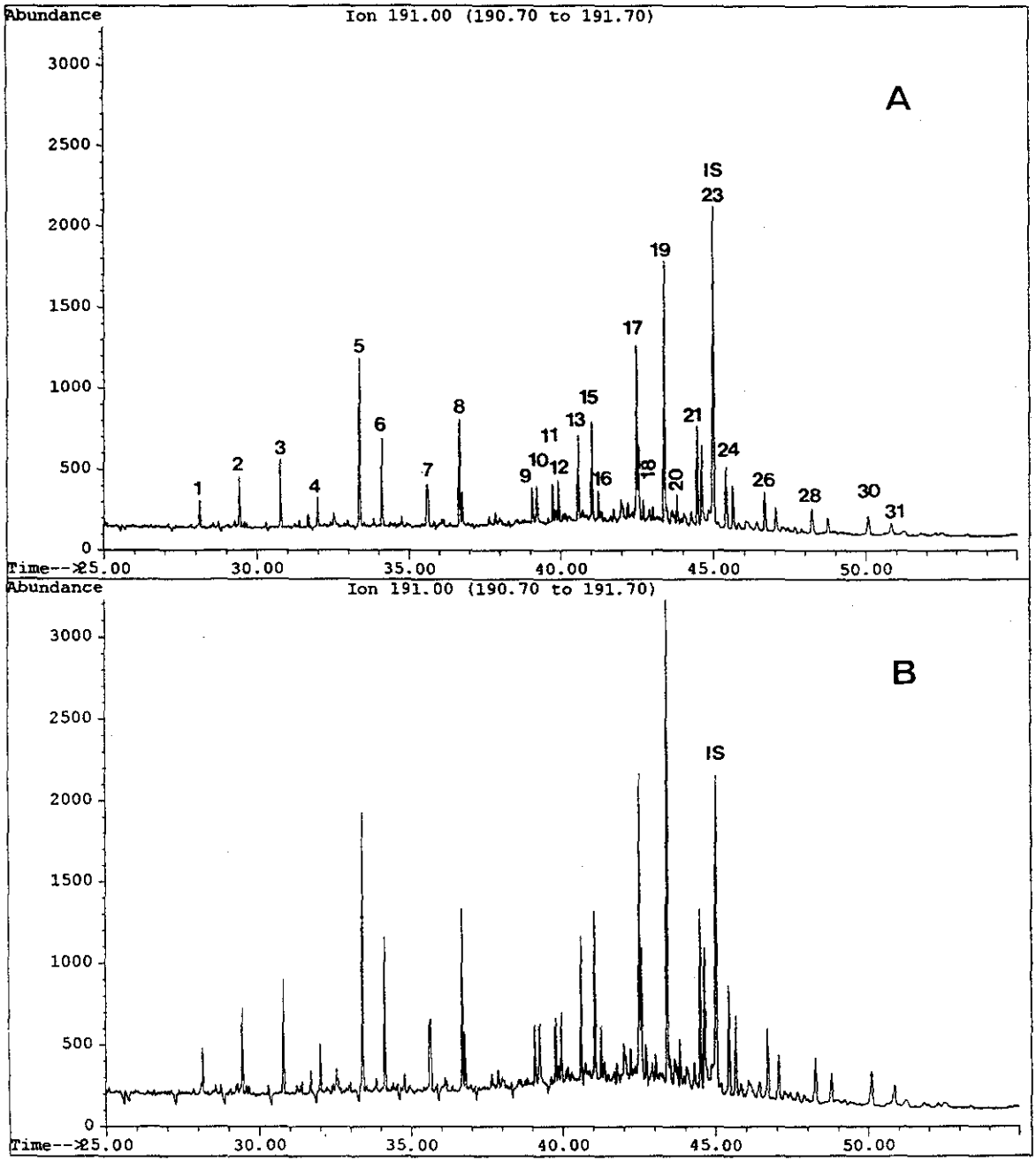

Figure 9. *Distribution of triterpanes (m / z 191 mass fragmentogram) of 0% (top) and 44.5% (bottom) weathered ASMB oil. The numbers above peaks represent the identified triterpanes (see Table IV for the chemical names of the identified components).*

Equation (3) implies that the evaporation percentages of the oil can be determined by quantifying the selected compounds in the weathered samples which are not lost during the weathering process, and by comparison with the concentrations of the corresponding compounds in the source oil.

Three weathered ASMB oil samples which were randomly collected from the pan evaporation process were analyzed together with the original ASMB oil and the results were compared with those found by gravimetric method. Thirteen target compounds and compound classes were quantified and their concentra-

Table IV. *Measured concentrations of triterpanes in weathered ASMB oil (μg / g oil).*

	Measured concentration (Cdet)					
	0%	9.80%	19.50%	29.80%	34.50%	44.50%
Tricyclic terpanes						
1 C19 tricyclic terpane	14.6	15.6	17.5	19.8	21.6	26.4
2 C20 tricyclic terpane	26.2	26.4	28.8	33.6	37.6	44.6
3 C21 tricyclic terpane	31.2	32.2	35.0	41.6	42.6	51.3
4 C22 tricyclic terpane	17.6	18.7	23.3	24.5	25.3	32.6
5 C23 tricyclic terpane	80.1	82.6	94.5	102.8	117.3	143.6
6 C24 tricyclic terpane	41.6	41.8	48.8	52.4	58.5	71.0
7 C25 tricyclic terpane	38.1	42.6	45.6	50.8	55.6	66.2
8 C26 tricyclic terpane	53.2	54.1	58.4	65.9	74.3	86.2
Tetracyclic terpanes						
9 C27 tetracyclic terpane	37.5	41.7	47.7	51.6	53.7	69.7
10 C27 tetracyclic terpane	(peak 9 +10)	(peak 9 +10)	(peak 9 +10)	(peak 9 +10)	(peak 9 +10)	(peak 9 +10)
11 C28 tetracyclic terpane	38.7	41.9	45.5	52.3	53.5	68.4
12 C28 tetracyclic terpane	(peak 11 + 12)	(peak 11 + 12)	(peak 11 + 12)	(peak 11 + 12)	(peak 11 + 12)	(peak 11 + 12)
Pentacyclic triterpanes						
13 Ts: 18α(H),21β(H)-22,29,30-trisnorhopane($C_{27}H_{46}$)	40.00	41.1	45.3	51.4	56.6	69.1
14 17α(H),18α(H),21β(H)-25,28,30-trisnorhopane($C_{27}H_{46}$)				(not quantified)		
15 Tm: 17α(H),21β(H)-22,29,30-trisnorhopane($C_{27}H_{46}$)	50.1	52.7	57.8	64.3	72.3	86.1

16 17α(H),18α(H),21β(H)-28,30-bisnorhopane($C_{28}H_{48}$)	13.1	15.1	17.5	17.0	19.5	22.7
17 C29 17α(H),21β(H)-30-norhopane	87.8	95.0	102.5	117.9	129.3	154.8
18 C29 18α(H),21β(H)-30-norneohopane				(not quantified)		
19 C30 17α(H),21β(H)-hopane	127.9	145.5	160.8	181.0	190.0	229.0
20 C30 17β(H),21α(H)-hopane	171.1	178.8	20.0	23.3	23.3	27.3
	Measured concentration (Cdet)					
	0%	9.80%	19.50%	29.80%	34.50%	44.50%
21 C31 22S-17α(H),21β(H)-30-homohopane	52.9	59.0	64.8	71.0	76.4	93.5
22 C31 22R-17α(H),21β(H)-30-homohopane	42.6	46.2	53.0	54.7	58.8	75.8
23 C30 17β(H),21β(H)-hopane				Internal Std.		
24 22S-17α(H),21β(H)-30,31-bishomohopane	42.0	45.1	50.5	56.5	59.1	73.6
25 22R-17α(H),21β(H)-30,31-bishomohopane	29.4	31.6	34.7	38.2	40.9	50.3
26 22S-17α(H),21β(H)-30,31,32-trishomohopane	27.5	32.0	34.7	39.6	38.8	50.5
27 22R-17α(H),21β(H)-30,31,32-trishomohopane	19.2	22.2	23.9	26.3	26.9	33.6
28 22S-17α(H),21β(H)-30,31,32,33-tetrakishomohopane	21.9	25.1	29.1	29.9	32.1	38.2
29 22R-17α(H),21β(H)-30,31,32,33-tetrakishomohopane	12.1	13.7	15.5	17.0	18.0	21.4
30 22S-17α(H),21β(H)-30,31,32,33,34-pentakishomohopane	18.3	21.2	24.8	26.5	29.0	33.9
31 22R-17α(H),21β(H)-30,31,32,33,34-pentakishomohopane	11.5	13.5	15.9	16.1	17.1	22.8
Total	991.5	1073.7	1195.4	1325.4	1427.7	1741.9

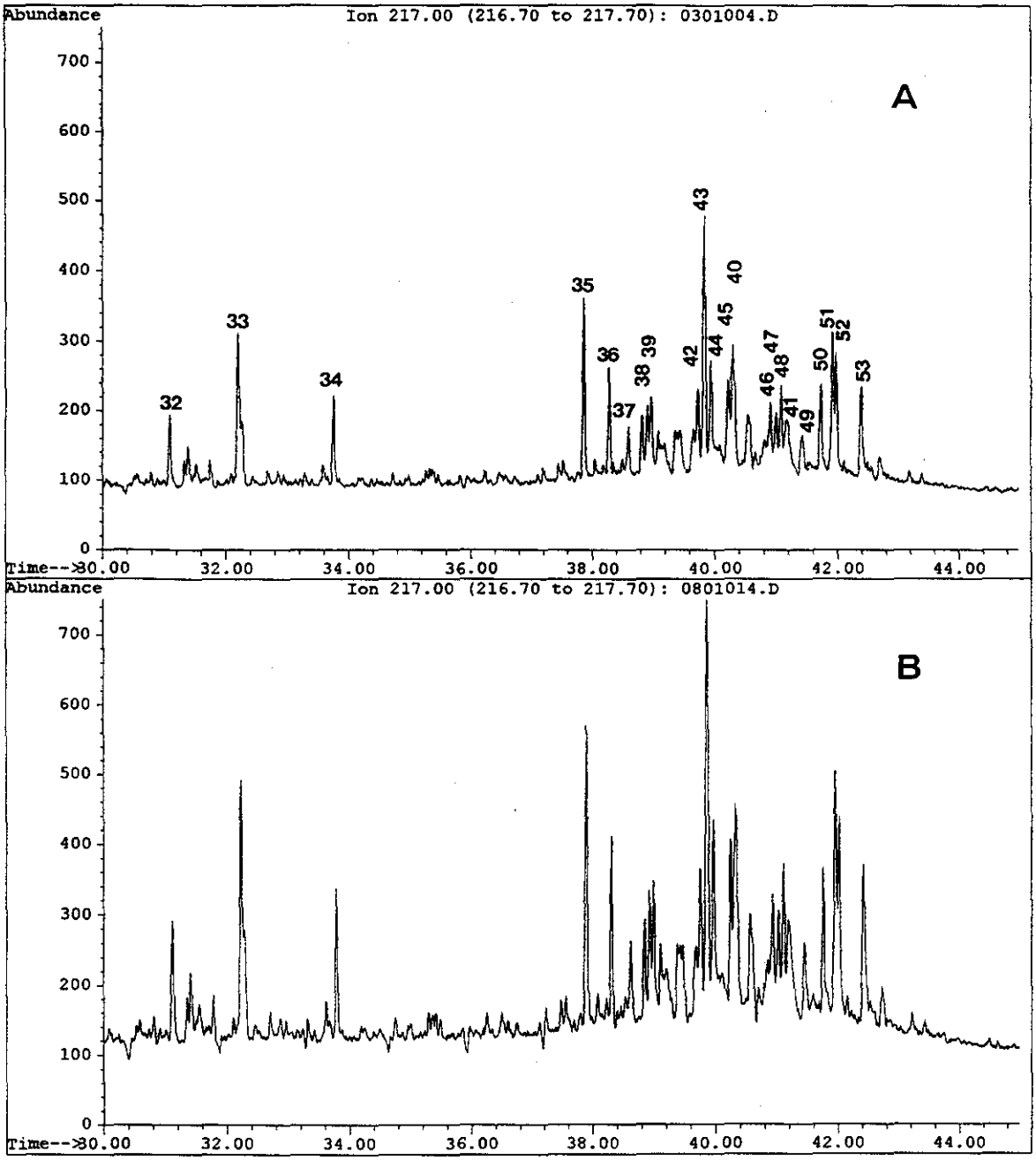

Figure 10. *Distribution of steranes (m / z 217 mass fragmentogram) of 0% (top) and 44.5% (bottom) weathered ASMB oil. The numbers above peaks represent the identified steranes (see Table 5 for the chemical names of the identified components).*

tions were used to determine the weathered percentages by using equation (3). Table VII summarizes the quantitation results. The average values of weathered percentages are determined to be 26.9 ± 2.0%, 34.3 ± 1.4%, and 40.3%2.1% for weathered samples 1, 2, and 3, respectively. The corresponding values obtained by the gravimetric method are 25.9%, 33.6%, and 38.6%. Clearly, these two sets of results from two totally different methods are in good agreement.

CONCLUSIONS

The effects of evaporation on oil composition was studied. The conclusions of this study are summarized as follows:

1. The key to acquiring data on oil weathering is the availability of precise and reliable

Table V. *Measured concentrations of steranes in weathered ASMB oil (μg / g oil).*

		Determined concentration (Cdet)					
		0%	9.8%	19.5%	29.8%	34.5%	44.5%
	Steranes						
32	C20 5α(H),14α(H),17α(H)-sterane	14.3	14.9	16.1	17.9	19.6	23.8
33	C21 5α(H),14β(H),17β(H)-sterane	31.8	32.8	35.2	41.5	44.7	53.5
34	C22 5α(H),14β(H),17β(H)-sterane	14.2	15.0	16.1	19.1	20.5	24.1
35	C27 20S-13β(H),17α(H)-diasterane	31.8	33.7	37.5	42.8	47.3	55.0
36	C27 20R-13β(H),17α(H)-diasterane	18.0	19.5	22.4	25.2	28.4	32.4
37	C27 20S-13α(H),17β(H)-diasterane			(not quantified)			
38	C27 20R-13α(H),17β(H)-diasterane			(not quantified)			
39	C28 20S-13β(H),17α(H)-diasterane			(not quantified)			
40	C29 20S-13β(H),17α(H)-diasterane			(not quantified)			
41	C29 20R-13α(H),17β(H)-diasterane			(not quantified)			
42	C27 20S 5α(H),14α(H),17α(H)-cholestane	20.5	23.5	26.2	26.3	25.1	34.7
43	C27 20R 5α(H),14β(H),17β(H)-cholestane	55.2	59.7	67.4	72.3	77.4	96.5
44	C27 20S 5α(H),14β(H),17β(H)-cholestane	29.3	31.7	37.6	39.4	42.2	50.8
45	C27 20R 5α(H),14α(H),17α(H)-cholestane	21.6	23.4	26.4	29.2	30.2	35.3
46	C28 20S 5α(H),14α(H),17α(H)-ergostane	20.0	20.3	22.2	24.4	27.6	30.6
47	C28 20R 5α(H),14β(H),17β(H)-ergostane	15.8	17.1	20.6	21.4	22.6	27.4
48	C28 20S5α(H),14β(H),17β(H)-ergostane	19.4	20.8	23.7	26.5	28.3	33.5
49	C28 20R 5α(H),14α(H),17α(H)-ergostane	13.3	13.6	16.6	17.4	18.7	22.6
50	C29 20S 5α(H),14α(H),17α(H)-stigmastane	21.0	22.9	26.9	28.1	30.0	37.2
51	C29 20R 5α(H),14β(H),17β(H)-stigmastane	28.2	30.5	35.0	36.7	40.5	52.2
52	C29 20S 5α(H),14β(H),17β(H)-stigmastane	22.6	24.8	30.1	31.0	33.3	42.3
53	C29 20R 5α(H), 14α(H),17α(H)-stigmastane	20.0	22.6	25.9	27.4	29.1	34.9
	Total	396.6	426.4	485.4	526.4	565.1	686.3

Table VI. *Relative ratios of triterpanes and steranes at six weathering degrees of ASMB oil.*

	Hopanes								
% weathered	C23/C24	Ts/Tm	C29aβ/ C30aβ	C31 S/ (S + R)	C32 S/ (S + R)	C33 S/ (S + R)	C34 S/ (S + R)	C35 S/ (S + R)	C31-C35 S/ (S + R)
0.0	1.92	0.80	0.69	0.55	0.59	0.59	0.64	0.61	0.60
9.8	1.98	0.78	0.65	0.56	0.59	0.59	0.65	0.61	0.60
19.5	1.94	0.78	0.65	0.55	0.59	0.59	0.65	0.61	0.60
29.8	1.96	0.80	0.65	0.56	0.60	0.60	0.64	0.62	0.60
34.5	2.00	0.78	0.68	0.57	0.59	0.59	0.64	0.63	0.60
44.5	2.02	0.80	0.69	0.55	0.60	0.60	0.64	0.61	0.60

	Steranes					
% weathered	20S(20S + 20R)			aββ/(aββ + aaa)		
	C27	C28	C29	C27	C28	C29
0.0	0.37	0.58	0.45	0.67	0.51	0.55
9.8	0.40	0.57	0.47	0.66	0.53	0.55
19.5	0.40	0.55	0.48	0.67	0.53	0.55
29.8	0.39	0.57	0.48	0.67	0.53	0.55
34.5	0.39	0.57	0.48	0.67	0.52	0.55
44.5	0.39	0.56	0.48	0.68	0.53	0.57

Table VII. *Determination of weathered percentages of weathered ASMB oil samples.*

Target Compounds	% weathered (determined by equation 3)* Sample 1	Sample 2	Sample 3
n-C26	27.6	35.5	40.4
n-C27	27.5	35.6	40.3
n-C28	26.2	33.7	38.4
n-C29	25.1	33.0	38.5
n-C30	25.5	34.2	39.6
C2-P	28.7	33.8	39.2
C3-P	26.5	35.8	40.0
C2-D	28.6	35.9	42.0
C3-D	31.6	35.1	43.0
C23-triterpane	23.4	33.1	40.0
Ts	25.6	31.1	42.0
Tm	26.9	35.4	44.0
C30 a β-hopane	26.7	34.2	36.1
Average (%)	26.9 $\pm$ 2.0	34.3 $\pm$ 1.4	40.3 $\pm$ 2.1
Weathered Percentage (%) (Gravimetrically Determined)	25.9	33.6	38.6

*P and D represent phenanthrene and dibenzothiophene, respectively.

chemical data. These data are essential to fully understand the fate and behavior of oil in the environment, to predict oil property changes and the concentration of toxic components remaining in the oil, and to construct useful oil spill models. This study provides an effective means to obtain such information.

2. This study correlates the degree of evaporation to the chemical composition changes of the oil. The chemical changes as the oil evaporated were documented within component classes (such as n-alkanes, alkylated PAHs, and biomarker compounds), between component classes (such as n-alkanes and isoprenoids, alkyl naphthalenes and alkyl phenanthrenes), and within isomeric mixtures (such as methyldibenzothiophenes).
3. The distribution of selected n-alkanes, alkylated aromatics, and triterpanes and steranes offers unique, sensitive and relatively stable fingerprints for examining the evaporation behavior of oil in the environment. The "pattern recognition" plots involving more than 100 important individual oil components and component groupings would permit deduction of a best set of values for exposure to evaporative weathering. It should be noted that there are two opposing effects during evaporation: one is the loss of oil components due to evaporation, and another is build-up of oil components due to volume reduction. The complex behavior of some components and component groups during weathering can be explained as the results of the combination of these two opposing effects.
4. The mathematical equations derived from this work are relatively simple and very useful. They can be utilized to estimate the evaporative loss or weather ing degree of oil.
5. To increase the reliability of determination of weathered percentages, multiple fingerprints should be considered and the concentration changes of multiple target components and component classes should be calculated not only relative to themselves but also in the overall context of the oil composition change.
6. It should be possible in principle to use the comprehensive information about chemical composition changes of oil as the oil weathering degrees change, such as shown in this study, to construct a relatively simple model with oil weathering predictive capability. In order to achieve this ultimate goal, more studies on weathering of various oils are being conducted in this laboratory to apply

the method presented in this work and other methods to best correlate the oil chemical composition and property changes to evaporation, dissolution, and even biodegradation and photooxidation.

ACKNOWLEDGMENT

The authors would like to thank Mr. Stephen Whiticar for his help in processing the weathering of the ASMB oil, and to Mrs. Lise Sigouin for the assistance in drawing of figures and tables. We also thank Mr. Michael Landriault for performing the cleanup of three weathered ASMB oil samples.

REFERENCES

1. R. E. Jordan and J. R. Payne, *Fate and Weathering of Petroleum Spills in the Marine Environment: A Literature Review and Synopsis*, (Ann Arbor Science Publishers, Ann Arbor, Michigan) (1980).
2. J. R. Payne and G. D. McNabb, Jr., *Marine Technology Society Journal*, **18**(3), 24–42, (1984).
3. C. D. McAuliffe, *1989 Oil Spill Conference*, San Antonio, Texas, pp. 357–363 (1989).
4. P. D. Boehm, D. L. Fiest, D. Mackay, and S. Paterson, *Environ. Sci. Technol.*, **16**, 498–505 (1982).
5. C. D. McAuliffe, In *Proceedings of Symposium on Fate and Effects of Petroleum Hydrocarbons in Marine Ecosystems and Organisms*, D. A. Wolfe, et al., Eds., (Pergamon Press, Elmsford, New York, 1977), pp. 363–372.
6. R. G. Riley, B. L. Thomas, J. W. Anderson, and R. M. Bean, *1980-81 Marine Environmental Research*, Vol. 4, pp. 109–119.
7. R. J. Law, *The Science of The Total Environment*, **15**, 37–49 (1980).
8. C. D. McAuliffe, J. C. Johnson, S. H. Greene, G. P. Canevari, and T. D. Searl, *Environ. Sci. Technol.*, **14**, 1509–1518 (1980).
9. P. D. Boehm and D. L. Fiest, *Environ. Sci. Technol.*, **16**, 67–74 (1982).
10. M. Fingas, "*Evaporation of Crude Oil Spills*," J. Hazardous Materials (in press, 1995).
11. Z. D. Wang, M. Fingas, and K. Li, *J. Chromatogr. Sci.*, **32**, 361–366 (1994).
12. Z. D. Wang, M. Fingas, and K. Li, *J. Chromatogr. Sci.*, **32**, 367–382 (1994).
13. Z. D. Wang, M. Fingas, and G. Sergy, *Environ. Sci. Technol.*, **28**(9), 1733–1746 (1994).
14. Z. D. Wang and M. Fingas, "Analysis Results of Water Samples and Residue Samples From Newfoundland Offshore Oil Burn Experiments," (internal report), Environment Canada, Ottawa (1994).
15. Z. D. Wang, M. Fingas, M. Landriault, L. Sigouin, and N. Xu, *Anal. Chem.* **67**, 3491–3500 (1995).
16. Z. D. Wang, M. Fingas, and G. Sergy, *Environ. Sci. Technol.* **29**, 2622–2631 (1995).
17. Z. D. Wang and M. Fingas, *Environ. Sci. Technol.* **29**, 2842–2849 (1995).
18. O. Grahl-Nielsen and T. Lygre, *Mar. Pollut. Bull.*, **21**, 176–183 (1990).
19. D. S. Page, J. C. Foster, P. M. Fickeett, and E. S. Gilfillan, *Mar. Pollut. Bull.*, **19**, 107–115 (1988).
20. S. D. Killops and V. J. Howell, *Chemical Geology*, **91**, 65–79 (1991).
21. E. T. Bulter, G. S. Douglas, and W. G. Steinhauter, In *On-site Bioreclamation*; R. E. Hinchee and R. F. Olfenbuttel, Eds. (Butterworth-Heineman Publishers, Stoneham, MA, 1991), pp. 515–521.
22. K. A. Kvenvolden, F. D. Hostettler, J. B. Rapp, and P. R. Carlson, *Mar. Pollut. Bull.*, **26**, 24 (1993).
23. J. A. Butt, D. F. Duckworth, and S. G. Perry, *Characterization of Spilled Oil Samples*, (John Wiley & Sons, New York, 1986).
24. F. Brakstad and O. Grahl-Nielsen, *Mar. Pollut. Bull.*, **19**, 319–324 (1988).
25. J. K. Valkman, R. Alexander, and R. I. Kagi, *Geochim. Cosmochim. Acta*, **47**, 1033–1040 (1983).
26. G. S. Douglas, *The Use of Hydrocarbon Analyses for Environmental Assessment and Remediation*, in *Contaminated Oils, Diesel Fuel Contamination*, P. T. Kostecki and E. J. Calabrese, Eds. (Lewis Publishers, Ann Arbor, MI, 1992), Chapter I.

Received: May 11, 1995
Accepted: August 21, 1995